

MUHAMMAD ADAM¹, ASRI JAYA², MUSRI MAWALEDA², IRZAL NUR³

Geology and characteristics of epithermal gold mineralization at the Motongkad Prospect, North Sulawesi, Indonesia

Introduction

In the Motongkad prospect, East Bolaang Mongondow Regency, North Sulawesi Province, Indonesia, an epithermal gold mineralization occurred, hosted in andesitic-basaltic breccia, lava and tuff members of the middle Miocene volcanic rock (*Tmv*). The volcanic rock is intruded by andesite dikes and contains fine quartz veins. Gold, silver, and pyrite are found in the quartz veins (Effendi and Bawono 1997). Geographically, the Motongkad prospect is included in the northern arm of the Sulawesi mineralization districts, which is a part of the Tertiary Western Sulawesi and the Quaternary Minahasa-Sangihe volcanic. Geologically, this region is rich in various types of mineral deposits. Mineralization that

✉ Corresponding Author: Muhammad Adam; e-mail: adammuh1974@gmail.com

¹ Earth and Environmental Technology Study Program, Geological Engineering Department, Faculty of Engineering, Hasanuddin University, Gowa, Indonesia; e-mail: adammuh1974@gmail.com

² Earth and Environmental Technology Study Program, Geological Engineering Department, Faculty of Engineering, Hasanuddin University, Gowa, Indonesia

³ Mining Engineering Department, Faculty of Engineering, Hasanuddin University, Gowa, Indonesia; e-mail: irzal.nur@eng.unhas.ac.id



© 2024. The Author(s). This is an open-access article distributed under the terms of the Creative Commons Attribution-ShareAlike International License (CC BY-SA 4.0, <http://creativecommons.org/licenses/by-sa/4.0/>), which permits use, distribution, and reproduction in any medium, provided that the Article is properly cited.

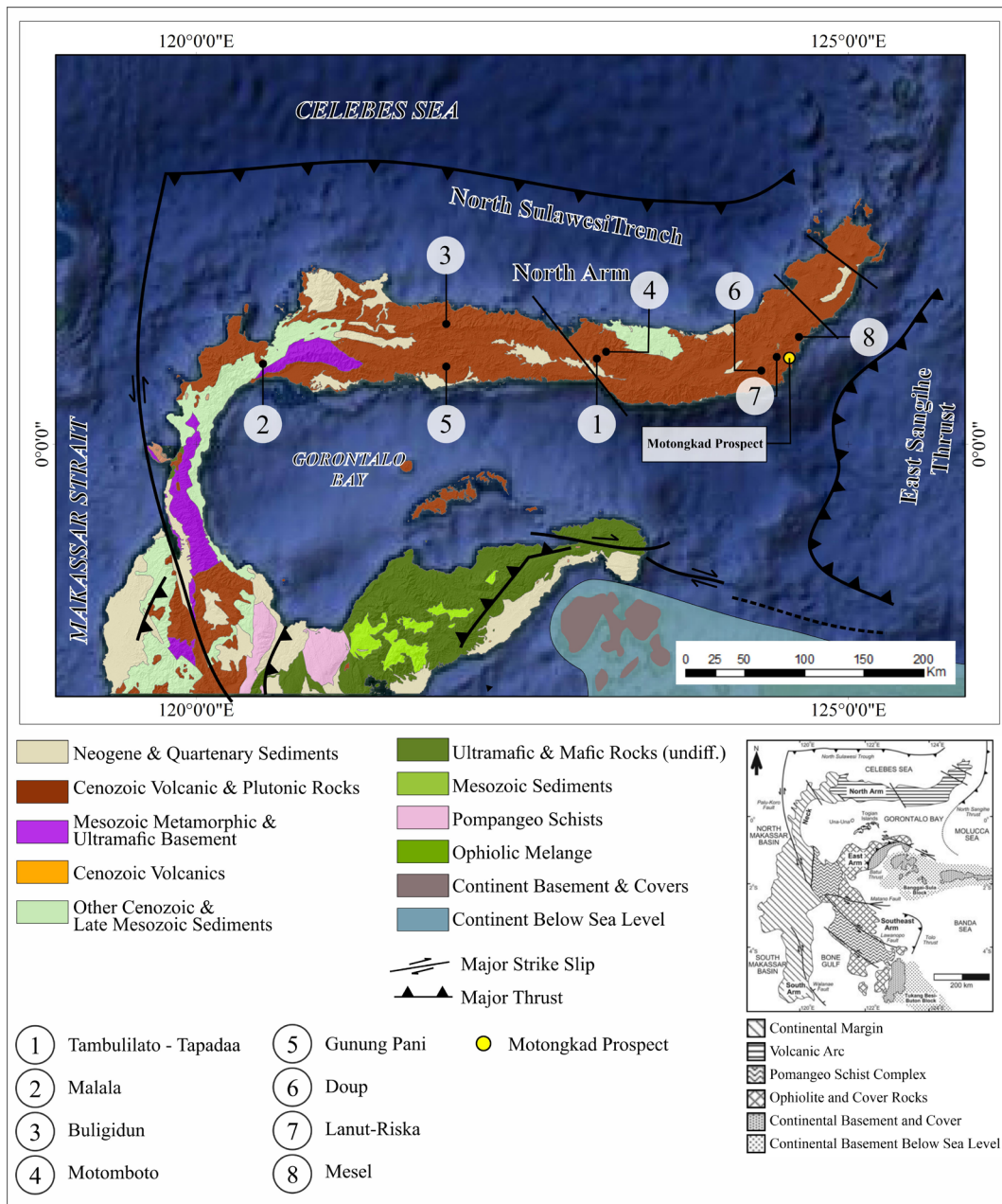


Fig. 1. Distribution of mineralization districts in the regional geology and lithotectonic map of the Northern Arm of Sulawesi showing the studied area (yellow point) (after Kavalieris et al. 1992; Hall and Wilson 2000)

Rys. 1. Rozmieszczenie rejonów mineralizacji na regionalnej mapie geologicznej i litotektonicznej północnego rejonu Sulawesii z zaznaczonym badanym obszarem (żółty punkt)

has been recognized and reported in this region include porphyry Cu-Au±Mo; high-, intermediate- and low-sulphidation epithermal Au-Ag; sediment hosted-Au; breccia-hosted base metal-Au; intrusion-related base metal-Au veins; Fe±Au skarns; and Cu-Pb-Zn volcanogenic massive sulphides (VMS), which are commonly formed during the Miocene period, particularly in the Pliocene magmatism period (van Leeuwen and Pieters 2011, 2012). At least eight mineralization districts in the northern arm of Sulawesi, namely Tambolilato-Tapadaa, Malala, Buligidun, Motomboto, Gunung Pani, Doup, Lanut-Riska and Mesel. The study area, the Motongkad prospect, is geographically adjacent to the Doup dan Lanut-Riska districts, which are Au-Ag epithermal high- to intermediate sulphidation types (Kavalieris et al. 1992).

This paper describes an update study of the epithermal gold mineralization in the Motongkad prospect based on recent field and laboratory data, which focused on its geology, hydrothermal alteration, ore and gangue mineralogy, as well as its chemical characteristics, to elucidate in more detail the specific type of the mineralization.

1. Methods

This study consists of two main stages, field works and laboratory works. The field works were performed in the whole area of the Motongkad prospect, where fresh and altered rock and mineralization samples were collected randomly, selectively, and systematically from outcrops as well as a test pit. The laboratory works include petrography, X-ray diffraction (XRD), ore microscopy, and chemical analysis using the atomic absorption spectrometry (AAS) method. Sample preparations for the microscopic studies, i.e., thin sections for petrography and polished sections for ore microscopy, as well as their observations using Nikon transmitted and reflected light microscope, were performed in the Optical Mineral Laboratory, Department of Geological Engineering, Hasanuddin University. For chemical analysis, mineralization samples were sent to be prepared in powder and analyzed by an atomic absorption spectrometry (ASS) method in a commercial research laboratory, PT. Intertek Utama Services, Jakarta, Indonesia.

2. Result and discussion

2.1. Local geology

The study area is arranged by three lithology units. Stratigraphically, the units are andesite, rhyolite, and tuff (the distribution and stratigraphic column are shown in Figure 2). The following sections describe characteristics of the three lithology units, from older to younger.

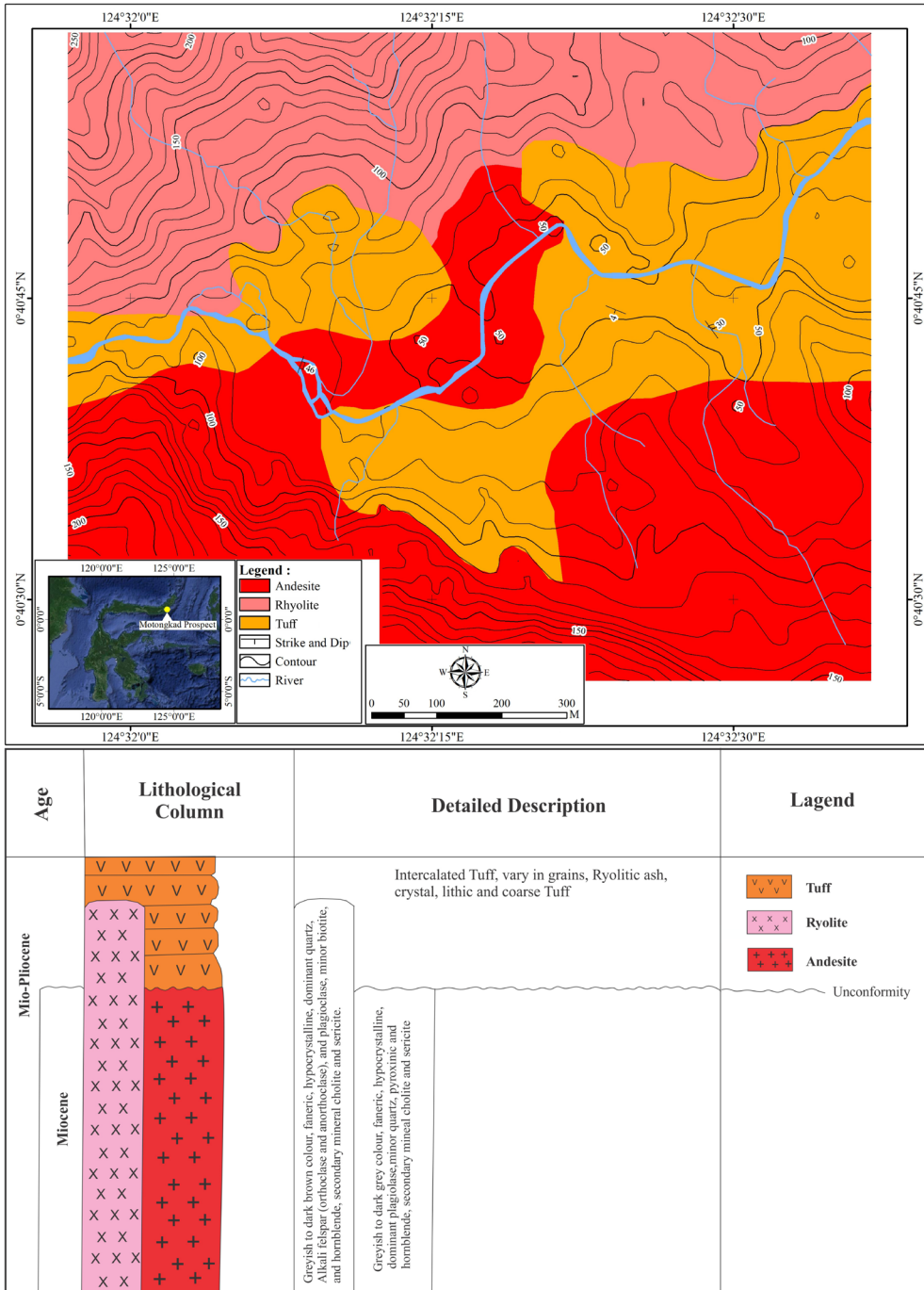


Fig. 2. A geological map and stratigraphic column of the study area

Rys. 2. Mapa geologiczna i kolumna stratygraficzna obszaru badań

2.1.1. Andesite

Andesite lava unit is widely distributed in the southern to the central part of the study area, occupying plains to hills morphology with elevations of 50 to 330 m. This unit consists of weakly to strongly altered andesite and andesite porphyry. In the field, andesite shows dark gray and partly greenish fine hypocrySTALLINE, with mineral composition of pyroxene, plagioclase, quartz, and ground mass. Quartz veinlet is found in the altered andesite.

2.1.2. Rhyolite

Rhyolite lava unit is distributed widely in the northern part of the study area, occupying hilly morphology, with elevations of 70 to 250 m. This unit is dominated by fine porphyritic rhyolite, which is weakly to strongly altered. In the hand specimen, rhyolite samples are gray to light gray in color, fine porphyritic and partly aphanitic, with mineral composition of quartz, feldspar, less biotite and hornblende, and fine microcrystalline as well as volcanic glass. In the field, vesicular rhyolite were also found.

2.1.3. Tuff

The tuff unit is distributed in a nearly west-east direction in the central part of the study area, occupying plains to hilly morphology with elevations of 30 to 100 m. This unit is mainly composed of rhyolitic tuff. Based on its bedding orientation which is measured in the field, where the strike is in the southwest-southeast orientation, the tuff is interpreted as the youngest unit of the three Volcanic Rocks (*Tmv*) in the study area. The tuff is strongly altered and contains mineralized quartz veins. In the upper part of the mineralized tuff, ± 2 m volcanic breccia found in the field its orientation is in the same direction as the vein, which is N292°E/4°. In the outcrops, tuff is brownish white in color and reddish brown when weathered indicating oxidation of its primary sulphides; it has a pyroclastic texture with <2 mm grain size, is well sorted and generally massive. While volcanic breccia is light brown to gray in color and dark brown when weathered; it is composed of mostly angular to less rounded fragments, is poorly sorted and sand to boulder size; it has composition of andesite, rhyolite, less dacite and basalt fragments, with volcanic ash matrix.

2.2. Hydrothermal alteration

Based on the alteration mineral assemblages identified under the microscope, the hydrothermal alterations in the study are grouped based on their domination and abundances as well as their location and distribution. In accordance with this, the hydrothermal alteration in the study area are classified in to five zones, namely: quartz-sericite, quartz-sericite-clay, quartz-calcite-sericite-chlorite, quartz-calcite-sericite, and quartz-calcite-kaolinite (Figure 3). The following sections the characteristics of each alteration zone.

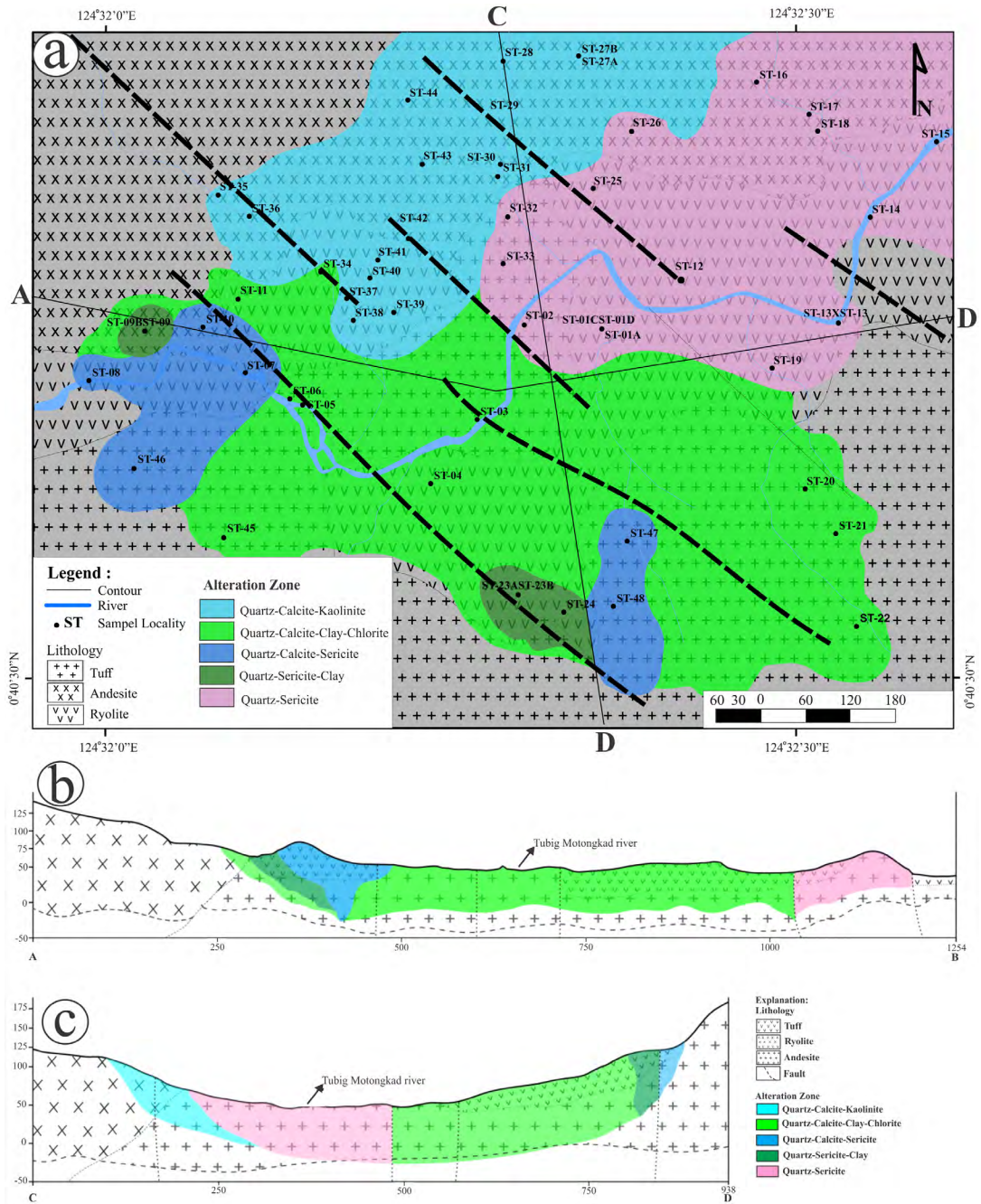


Fig. 3. a) Hydrothermal alteration map of the study area; b) Cross-section profile of line A-B; c) Cross-section profile of line C-D

Rys. 3. a) mapa zmian hydrotermalnych obszaru badań; b) profil przekroju linii A-B; c) profil przekroju linii C-D

2.2.1. Quartz-Sericite

Quartz-sericite is the widest alteration zone in the study area, which is distributed in the northeastern part (Figure 3). This alteration occurs in two types of rocks, tuff and porphyritic rhyolite. Observation under the microscope in altered tuff samples indicates a composition of quartz, sericite, illite, kaolinite and opaques. Coarse-grained opaques (0.10–0.35 mm), generally euhedral-cubic to subhedral, were interpreted as pyrite (Figure 4). Quartz, feldspar and illite were also identified by X-ray diffraction (XRD) (Figure 5a). Under the microscope, the altered porphyritic rhyolite samples show assemblages of quartz, sericite, less chlorite clay that have altered the primary minerals of feldspar and ground mass. The mineral composition is quartz, sericite, chlorite, clay, and opaques. Mineralization were also identified by the presence of cubic opaques which distributed associated with the alteration minerals (Figure 4).

2.2.2. Quartz-Sericite-Clay

This alteration zone is characterized by the presence and domination of quartz, sericite, and clay, which is distributed in the southern and western parts of the study area (Figure 3). This alteration occurs in two types of rocks, namely porphyritic rhyolite and rhyolitic tuff. Observation under the microscope in porphyritic rhyolite samples show a domination of very fine-grained clay, sericite replaced K-feldspar, microcrystalline (<0.2 mm) secondary quartz associated with opaques and filling fine veins, rhombohedral adularia disseminated among quartz crystals, fine-grained anhedral and coarse-grained subhedral opaques, and dendritic opaques. The mineral composition is quartz, sericite, clay, adularia and opaques (Figure 4). Pyrite and calcite were also identified by XRD (Figure 5b, 5c). Under the microscope the altered rhyolitic tuff samples show assemblages of quartz, sericite replaced feldspar in ground mass, very fine-grained clay filling open spaces, and granular (<0.01 mm) opaques. Sericite-silica-opaques were observed formed in the early phase then overprinted by clay-opaques (Figure 4). Quartz and feldspar were also identified by X-ray diffraction (XRD) analysis (Figure 5).

2.2.3. Quartz-Calcite-Sericite

The quartz-clacite-sericite zone is locally distributed in the western part of the study area, which trends northeast-southeast (Figure 3). This alteration occurs in three types of rocks, namely rhyolitic tuff, porphyritic rhyolite, and porphyritic andesite. Observation under the microscope generally shows alteration minerals of quartz and less sericite that altered primary feldspar and ground mass, calcite altered primary mafic minerals, clay, less epidote, and cubic to subhedral opaques (Figure 4). Quartz and feldspar, as well as pyrite were also identified by X-ray diffraction (XRD) analysis (Figure 5e).

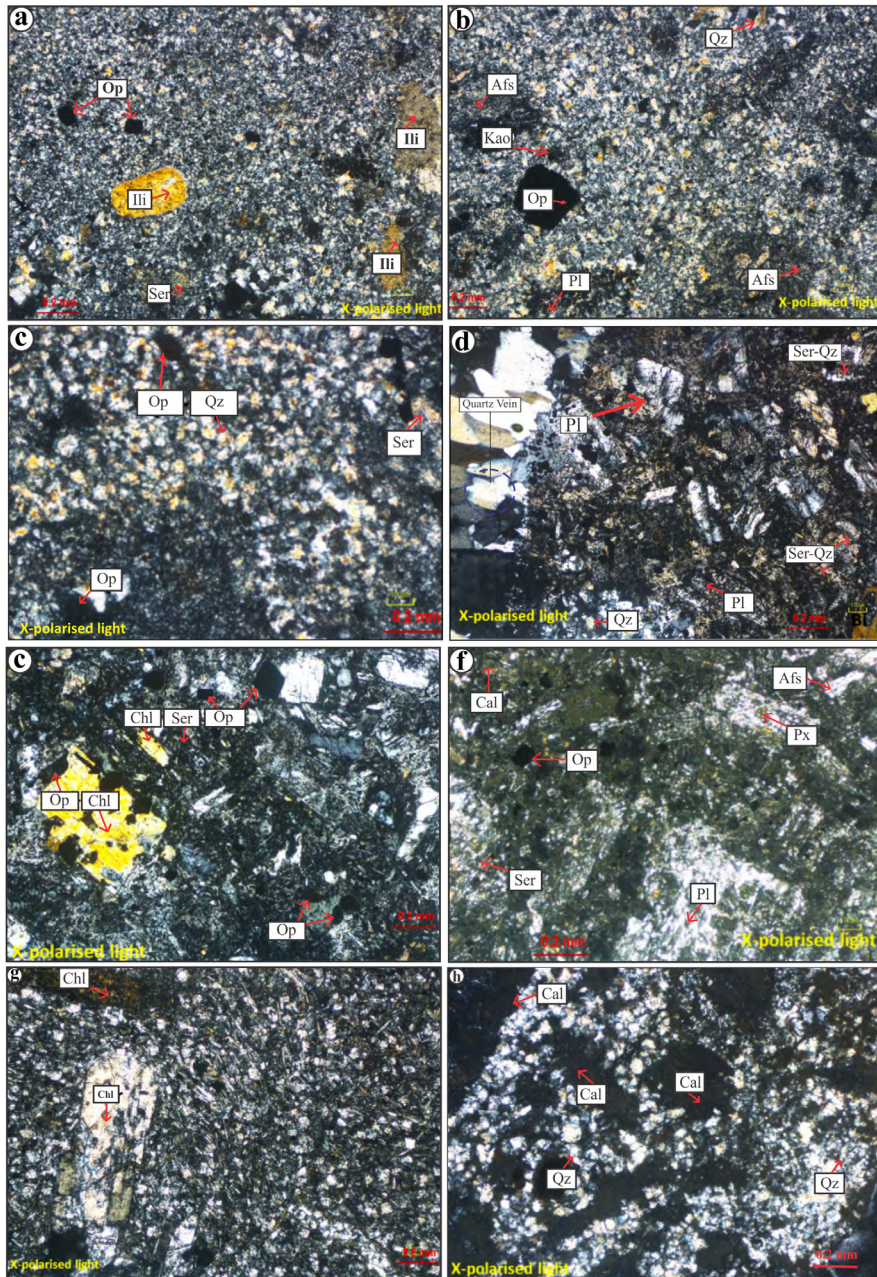


Fig. 4. Photomicrographs of alteration mineral assemblages described in Section 3a and 3b
 Ill – illite, Kao – kaolinite, Ser – sericite, Qz – quartz, Chl – Chlorite, Cal – calcite, Op – opaques.
 Relicts of primary minerals Kfs – K-feldspar and Pl – Plagioclase shown in Figure b and f

Rys. 4. Fotomikrografie przeobrażeń zespołów mineralnych opisanych w rozdziale 3a i 3b
 Ill – illit, Kao – kaolinit, Ser – serycyt, Qz – kwarc, Chl – chloryt, Cal – kalcyt, Op – nieprzezroczyste.
 Relikty minerałów pierwotnych Kfs – skałen K i Pl – plagioklaz pokazane na rys. b i f

2.2.4. Quartz-Calcite-Kaolinite

The quartz-calcite-kaolinite zone, locally distributed in the northern part of the study area (Figure 3), altered the porphyritic rhyolite lava. Under the microscope, kaolinite was observed which replaced the primary felsic phenocrysts in a pseudomorphic form; likewise with calcite-opaques. Recrystallization of quartz in the microcrystalline form, <0.03 mm in size, occurs in ground mass. The composition of the alteration minerals are quartz, calcite (fills 0.01–0.02 mm veins and in microcrystalline form replaces phenocryst), kaolinite, and <0.01 mm granular opaques (Figure 4). Quartz, feldspar, and kaolinite were identified by X-ray diffraction (XRD) analysis as shown in Figure 5F, while calcite is identified in Figure 5d.

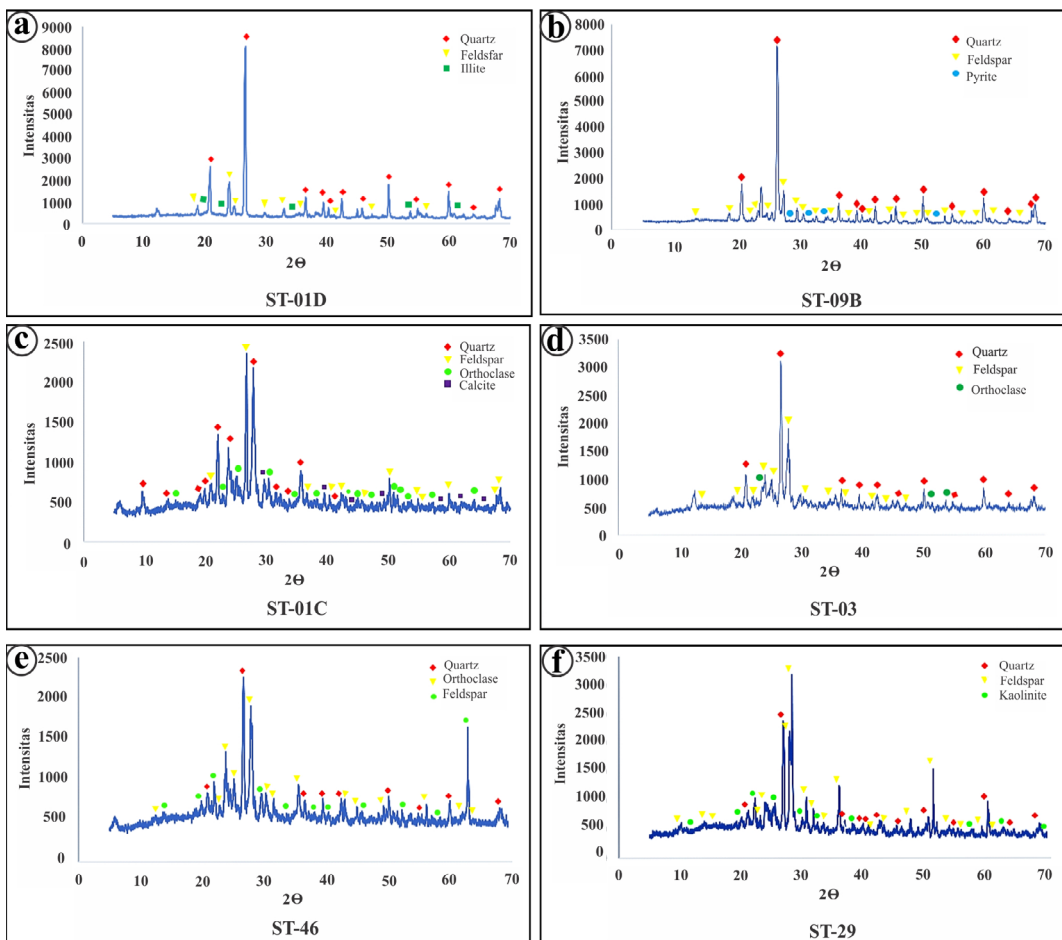


Fig. 5. X-Ray diffractograms show the alteration mineral assemblages described in section

Rys. 5. Dyfraktogramy rentgenowskie przedstawiają zmiany w zbiorowiskach minerałów opisane w rozdziale

2.3. Mineralization

In general, there are two types of mineralization in the study area, vein and dissemination. Quartz veins occurred in altered tuff, in the quartz-sericite zone, with nearly north-west-southeast strike and gently dip (N292°E/4°). Thin quartz and sulphide veins are commonly found (Figure 6a, 6b).

Under the microscope, polished sections show ore mineral assemblages of hypogene pyrite, sphalerite and chalcopyrite, as well as supergene covellite. Pyrite is mostly euhedral cubic to subhedral, some are scattered with sparse space (Figure 7a) and some are found with intergrowth texture with corroded sphalerite (Figure 7b). Chalcopyrite is generally anhedral, corroded, and replaced by covellite around their fringes (Figure 7a). Covellite also found on surfaces of subhedral pyrite (Figure 7d). Analysis using the atomic absorption spectrometry method indicates the highest grades of Au 0.19 ppm, Ag 47 ppm, Cu 78 ppm, Pb 11 ppm, and Zn 8 ppm.

Under the microscope, the Stockwork vein in altered porphyritic andesite (Figure 6f) shows mineral assemblage of pyrite, sphalerite, chalcopyrite and covellite. Paragenetically, pyrite is the earliest precipitated mineral. Sphalerite and chalcopyrite precipitated in the second phase, where sphalerite mostly fine grains and occupying the fringes of pyrite, while chalcopyrite are coarse grains, anhedral, and precipitated on the surface of pyrite (Figure 7b). Covellite is the last stage mineral (supergene), replaced chalcopyrite (Figure 8d). The ore grade is: Au 0.77 ppm, Ag <1 ppm, Cu 122 ppm, Pb 17 ppm, dan Zn 91 ppm.

Under the microscope, the vuggy quartz vein (Figure 6g) shows ore mineral assemblage of pyrite, sphalerite, chalcopyrite, covellite, chalcocite, and gold. Pyrite, chalcopyrite and sphalerite are coeval in intergrowth texture, as are the early phase minerals. Pyrite is mostly fine grain, euhedral to subhedral, and more disseminated, while chalcopyrite and sphalerite are generally coarse grain, and subhedral to anhedral (Figure 7c). Covellite and chalcocite are supergene minerals, where covellite replace chalcopyrite and chalcocite replace pyrite

Fig. 6. a) Outcrop of altered tuff with N292°E/4° quartz vein; b) sample of altered tuff containing thin quartz veins and fine grain sulfides on their both sides; c) mineralized-altered rhyolitic tuff outcrop; d) close-up of the outcrop in Photo A showing the silicification and oxidation zones; e) mineralized-altered rhyolitic tuff of containing quartz and sulfide veins; Au grade 0.83 g/t; f) Stockwork vein in altered porphyritic andesite; g) vuggy textured quartz veins in strongly altered porphyry rhyolite host rocks; h) altered porphyry andesite samples containing quartz veins and fine sulfide grains were dominated by pyrite

Rys. 6. a) Wychodnia tufu zmienionego z żyłą kwarcową N292°E/4°; b) próbka zmienionego tufu zawierająca po obu stronach cienkie żyłki kwarcu i drobnoziarniste siarczki; c) wychodnie tufu ryolitycznego o zmienionym zmineralizowaniu; d) zbliżenie wychodni na zdjęciu A pokazujące strefy krzemionkowania i utleniania; e) zmineralizowany tuf ryolitowy zawierający żyły kwarcowe i siarczkowe; gatunek Au 0,83 g/Mg; f) Żyła kolczasta w zmienionym porfirowym andezycie; g) żyły kwarcowe o nierównej teksturze w silnie zmienionych skałach macierzystych ryolitu porfirowego; h) próbki zmienionego porfirowego andezytu zawierające żyły kwarcowe i drobne ziarna siarczku były zdominowane przez pirit

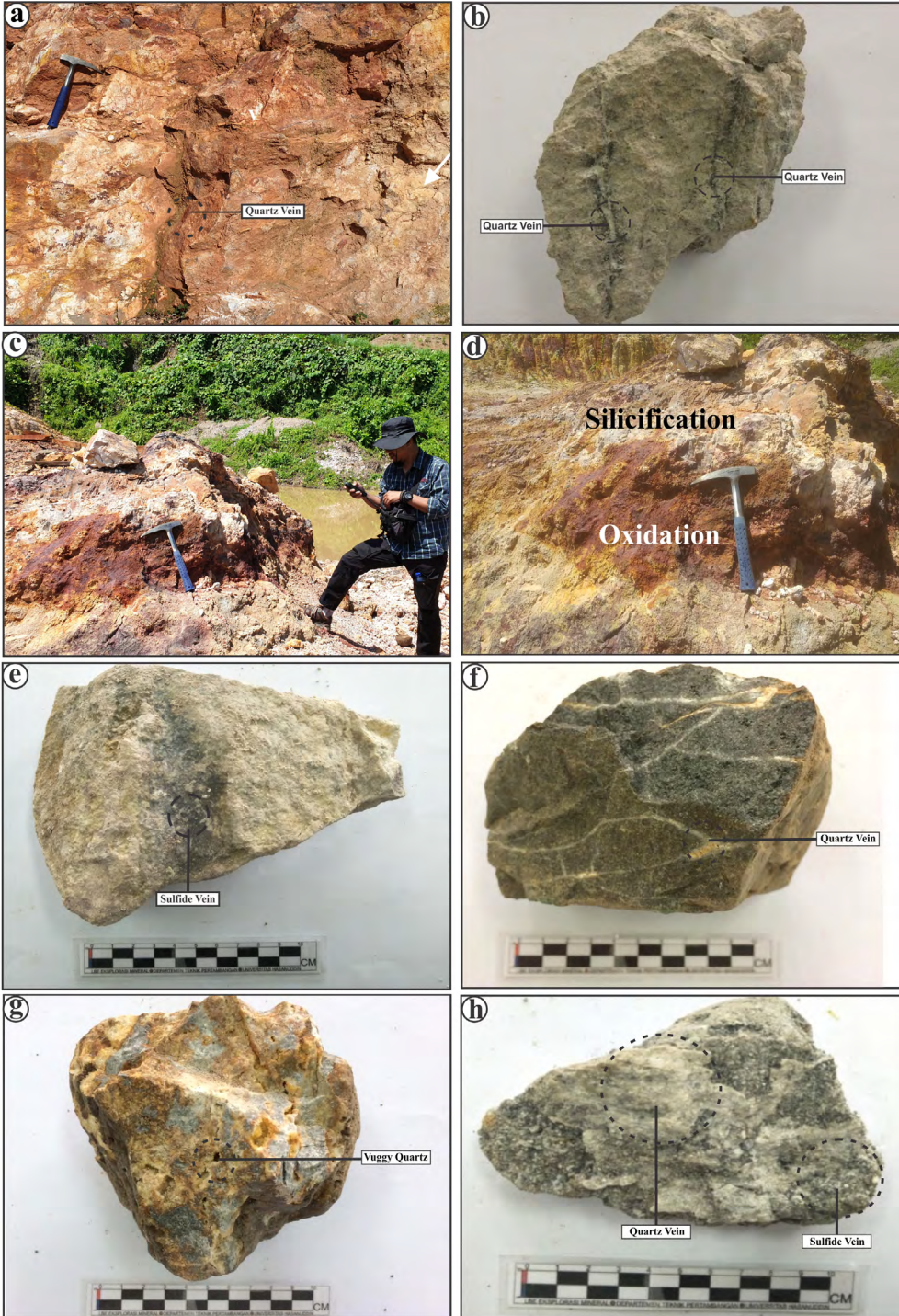


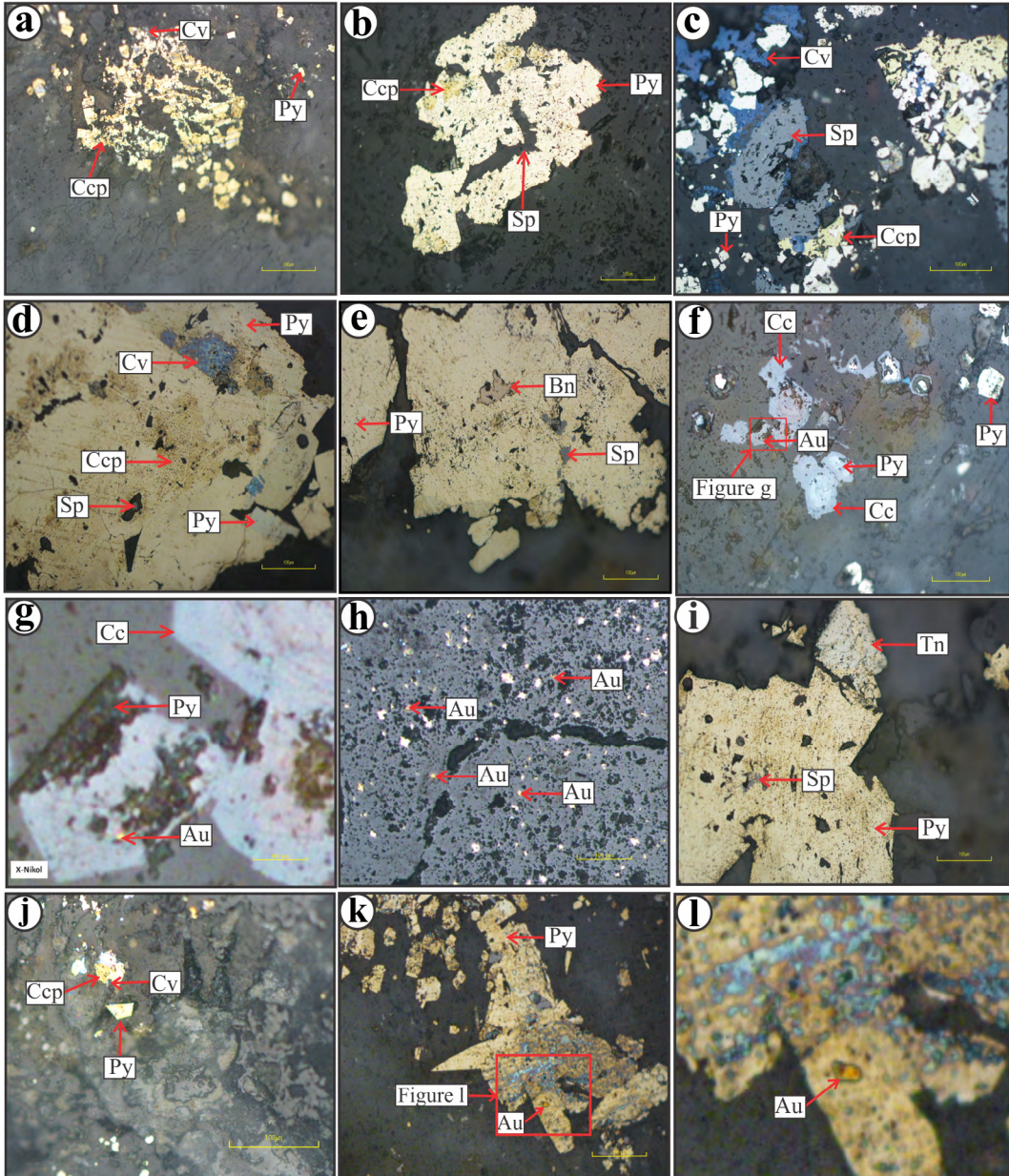
(Figure 7f). A very fine grain gold ($\pm 0.3 \mu\text{m}$) occurred as inclusion on corroded pyrite that has partly replaced by chalcocite (Figure 7g). Analysis using atomic absorption spectrometry (AAS) method indicates grades of: Au 1.07 ppm, Ag 5 ppm, Cu 337 ppm, Pb 331 ppm, and Zn 445 ppm. This mineralization with significant grade of gold and silver occurred in the quartz-sericite-clay alteration zone. In sample ST.11 (altered tuff containing fine-grained sulphides), under the microscope, fine pyrite grains were observed scattered in sparse space together with fine ($<0.1 \mu\text{m}$) gold grains (Figure 7h).

Observation under a microscope showed a set of hypogene pyrite ore minerals, chalcopyrite, sphalerite, and tennantite, as well as the supergene covellite and bornite minerals. The observed pyrite minerals dominate the rock samples and formed as early phase minerals,

- Fig. 7. a) Chalcopyrite generally anhedral, corroded, and replaced by covellite around their fringes; b) chalcopyrite are coarse grains, anhedral, and precipitated on surface of pyrite; c) pyrite are mostly fine grain, euhedral to subhedral, and more disseminated, while chalcopyrite and sphalerite are generally coarse grain, and subhedral to anhedral; d) chalcopyrite, sphalerite, and tennantite precipitated later, in smaller sizes, where chalcopyrite (up to 0.1 mm) and tennantite (0.01–0.02 mm in size) were observed over pyrite and sphalerite (0.01–0.05 mm in size) to fill the cracks/pores in pyrite; e) covellite and bornite are formed in the final stage, where both have replaced the chalcopyrite mineral in the pores/holes of pyrite mineral; f) covellite and chalcocite are supergene minerals, where covellite replace chalcopyrite; g) a very fine grain gold ($\pm 0.3 \mu\text{m}$) occurred as inclusion on corroded pyrite that has partly replaced by chalcocite; h) a very fine grain gold ($\pm 0.3 \mu\text{m}$) occurred as inclusion on corroded pyrite that has been partly replaced by chalcocite; i) pyrite dominated the samples and formed as early phase minerals, with fine to coarse (up to 0.2 mm) and euhedral to subhedral shapes; subhedral tennantite measuring 0.1–0.2 mm grows together with pyrite minerals; j) the chalcopyrite and sphalerite precipitated at a later stage, where sphalerite was observed fine in size on top of the pyrite; k) very fine-grained chalcopyrite ($<0.025\text{--}0.5 \text{ mm}$) was scattered sparsely spaced together with the sphalerite and fine-grained euhedral pyrite; l) we also found $\pm 10 \mu\text{m}$ refined gold grains (electrum) as inclusions in corroded subhedral pyrite.
- Au – Gold, Bn – Bornit, Ccp – Chalcopyrite, Cv – Covellite, Cc – Chalcocite, Py – Pyrite, Sp – Sphalerite, Tn – Tennantite

- Rys. 7. a) Chalkopiryt generalnie anhedralny, skorodowany i zastąpiony kowelit na obrzeżach; b) chalkopiryt jest gruboziarnisty, anhedralny i wytrąca się na powierzchni piryty; c) piryt jest przeważnie drobnoziarnisty, euhedralny do subhedralnego i bardziej rozproszony, podczas gdy chalkopiryt i sfaleryt są na ogół gruboziarniste i subhedralne do anhedralnych; d) chalkopiryt, sfaleryt i tennantyt wytrąciły się później, w mniejszych rozmiarach, gdzie nad pirytem i sfalerytem (o wielkości 0,01–0,05 mm) zaobserwowano chalkopiryt (do 0,1 mm) i tennanit (o wielkości 0,01–0,02 mm) w celu wypełnienia pęknięć/por w piryty; e) w końcowym etapie powstają kowelit i bornit, gdzie oba zastąpiły minerał chalkopiryty w porach/otworach minerału piryty; f) kowelit i chalkozyt są minerałami supergeny, gdzie kowelit zastępuje chalkopiryt; g) bardzo drobnoziarniste złoto ($\pm 0,3 \mu\text{m}$) występowało jako inkluzja na skorodowanym piryty, który został częściowo zastąpiony przez chalkozyt; h) bardzo drobnoziarniste złoto ($\pm 0,3 \mu\text{m}$) występowało jako inkluzja na skorodowanym piryty, który został częściowo zastąpiony przez chalkozyt; i) piryt dominował w próbkach, powstał jako minerały wczesnej fazy, o kształtach drobnych do grubych (do 0,2 mm) i euhedralnych do subhedralnych kształtach; subhedralny tennantyt o wymiarach 0,1–0,2 mm rośnie wraz z minerałami piryty; j) chalkopiryt i sfaleryt wytrąciły się w późniejszym etapie, gdzie na wierzchu piryty zaobserwowano drobny sfaleryt; k) bardzo drobnoziarnisty chalkopiryt ($<0,025\text{--}0,5 \text{ mm}$) był rozproszony w niewielkich odstępach razem ze sfalerytem i drobnoziarnistym pirytem euhedralnym; l) znaleziono również $\pm 10 \mu\text{m}$ rafinowane ziarna złota (elekttrum) jako wtrącenia w skorodowanym subhedralnym piryty.
- Au – złoto, Bn – bornit, Ccp – chalkopiryt, Cv – kowelit, Cc – chalkozyn, py – piryt, Sp – sfaleryt, Tn – tennantyt

generally coarse (up to 0.2 mm) in size and euhedral (cubic) to subhedral in shape. Chalcopyrite, sphalerite, and tennantite precipitated later, in smaller sizes, where chalcopyrite (up to 0.1 mm) and tennantite (0.01–0.02 mm in size) were observed over pyrite and sphalerite (0.01–0.05 mm in size) to fill the cracks/pores in pyrite (Figure 7d). In contrast, covellite and bornite are formed in the final (supergene) stage, where both have replaced the chalcopyrite



mineral (which is interpreted based on the relic anhedral shape) in the pores/holes of pyrite mineral (Figure 7e). The results of the atomic absorption spectrometry method analysis of this sample showed a significant Au content, namely 0.13 g/t (Table 1). However, we did not find gold-bearing minerals when conducting observations under a microscope; this may be due to their smaller size.

Table 1. Significant Au grades at Motongkad Prospect

Tabela 1. Znaczące klasy Au w Prospekcji Motongkad

No.	Location	Number Sample	Au (g/t)
1.	ST-01	ST-1A	0.91
2.	ST-03	ST-3	0.77
3.	ST-04	ST-4	0.42
4.	ST-09	ST-9B	1.07
5.	ST-13	ST-13A	0.13
6.	ST-13	ST-13B	0.13
7.	ST-23	ST-23A	0.85
8.	ST-23	ST-23B	0.88
9.	ST-24	ST-24	0.83
10.	ST-41	ST-41	0.46

Observation under a microscope reveals hypogene pyrite, chalcopyrite, sphalerite, tennantite and gold ore mineral assemblages, as well as supergene covellite minerals. Pyrite dominated the samples and formed as early phase minerals, with fine to coarse (up to 0.2 mm) and euhedral to subhedral shapes. Subhedral tennantite measuring 0.1–0.2 mm grows together with pyrite minerals (Figure 7i). The chalcopyrite and sphalerite precipitated at a later stage, where sphalerite was observed to be fine in size on top of the pyrite (Figure 7j) and very fine-grained chalcopyrite (<0.025–0.5 mm) was scattered sparsely spaced together with the sphalerite and fine-grained euhedral pyrite. The supergene covellite minerals were observed to replace the edges of these chalcopyrite crystals (Figure 7k). We also found $\pm 10 \mu\text{m}$ refined gold grains (electrum) as inclusions in corroded subhedral pyrite (Figure 7l).

Researchers made a test pit on altered porphyry andesite rock (Figure 6h). Samples of porphyry andesite rock that had been strongly altered and contained quartz vein mineralization were taken with a thickness of 2 cm, and the granules refined sulphide dominated by pyrite. Under the microscope, this ST.20 sample shows the assemblages of hypogene pyrite, chalcopyrite, sphalerite ore minerals, and supergene covellite minerals. As in other samples, pyrite appears to predominate in polishing sections and formed as early phase minerals, with fine to coarse (up to 0.2 mm) and euhedral to subhedral shapes. Fine-grained chalco-

pyrite and sphalerite (<0.025–0.5 mm) precipitated at a later stage, which appeared to be on top of the mineral pyrite. We found fine-grained chalcopyrite scattered with fine-grained subhedral pyrite, and some chalcopyrite has changed to supergene covellite minerals, especially at the edges. The results of chemical analysis using the atomic absorption spectrometry method showed insignificant ore content in this sample, namely Au <0.01 ppm and Ag <1 ppm (both were below the detection limit). The three base metal elements also have low grades: 9 ppm Cu, 5 ppm Pb, and 17 ppm Zn (Table 1). The location of disseminated sulphide mineralization and quartz veins in the altered porphyry andesite rock at ST.20 is in the quartz-calcite-sericite-chlorite alteration zone (Figure 3).

Based on the atomic absorption spectrometry (AAS) analysis results, several locations and samples in Prospect Motongkad showed a significant grade of Au and a relatively high increase in the grade of Ag. However, the overall grades of the base metals were low. As a reference, significant ore grades were assessed based on exploration results in the areas surrounding Prospect Motongkad, namely in the Lanut and Doup Mineralization Districts. In Lanut District, the minimum Au grade still considered is in the range (of 0.1–0.5) g/t, while in Doup District, it is (0.7–1.2 g/t). The minimum Ag grade in the Lanut district is 4.5 g/t. The minimum Cu grade in the Doup district (porphyry Cu-Au type mineralization) is 0.1% or 1000 g/t (van Leeuwen and Pieters 2011, 2012; Kavalieris et al. 1992). On this basis, we compiled tables and diagrams containing locations and samples of each considered to have significant Au grades (Table 1).

On the basis of Table 1 and Figure 8, we conclude that the range of significant Au grade in the study area is 0.13–1.07 g/t, with the highest range (above 0.8 g/t) being 0.83–1.07 g/t, namely in the samples ST-1A, ST-9B, ST-23A, ST-23B, and ST-24. The samples ST-1A and ST-9B are described with regard to their microscopic characteristics at the start of this chapter. The following paragraphs present a description of ST.23 and ST.24.

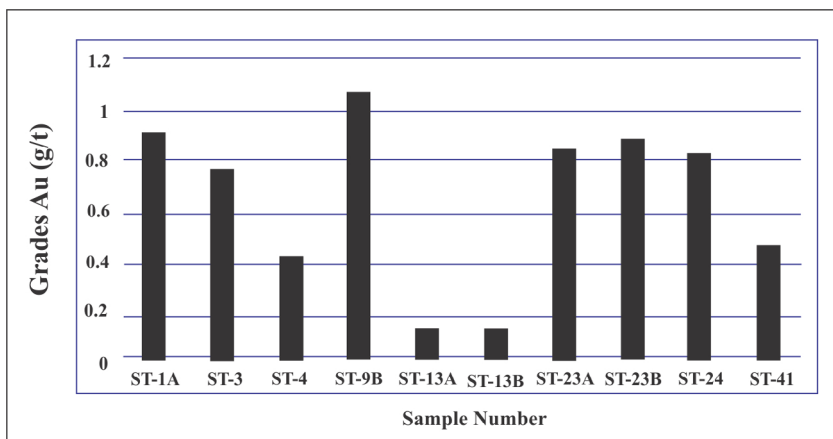


Fig. 8. Distribution of Au grades in significant mineralized samples in the Prospect Motongkad

Rys. 8. Rozkład klas Au w znaczących zmineralizowanych próbkach w prospekcje Motongkad

At location ST-23, we found outcrops of rhyolite tuff that had undergone intense alteration. Field identification showed intensive silicification alteration, and the outcrop surface showed a high oxidation level, characterized by a reddish-brown to red color, so we indicated weathering had occurred in the form of oxidation of the metal sulphide minerals they contain. Mineralized samples from this site also reveal 5 cm thick quartz and sulphide veins (Figure 6c, 6d, 6e).

At location ST.24, we also encountered the same type of mineralization: a strongly altered rhyolitic tuff containing quartz and oxidized sulphide veins, as seen in Figure 6. At locations ST-4 and ST-41, mineralized samples with significant Au levels were also found (Table 1). At ST-4, the mineralization is in the form of quartz veins on the altered tuff hosts found on the roadside cliffs. In the outcrop, these 10-cm-thick quartz veins show dog teeth and vuggy textures and have undergone partial oxidized (reddish-brown to red) indicating their sulphide content (Figure 6f). The Quartz vein samples taken from this location show a vuggy quartz texture with a vug diameter of up to 1 cm; indications of oxidation also appear on the sample surface (Figure 7b). The results of the atomic absorption spectrometry (AAS) method analysis on the ST.4 sample showed Au grades of 0.42 g/t and Ag 1 g/t, with low base metal content, namely: Cu 20 ppm, Pb <4 ppm (below the detection limit), and Zn 8 ppm (Table 1).

At location ST-41, we encountered very fine-grained disseminated sulphide mineralization in the altered tuff host in the 2 m bottomless test pit at this location. Sample ST-41 macroscopically showed refined sulphide grains tightly spaced to form separate clusters; quartz veins approximately 1.5 cm thick were also observed in this sample. The results of the atomic absorption spectrometry method analysis on the ST-41 sample showed an Au grade of 0.46 g/t, with a low content of silver and base metals, namely Ag <1 ppm (below the detection limit), Cu 16 ppm, Pb 13 ppm, and Zn 5 ppm (Table 1).

3. Prospect evaluation

Based on the results of the previous discussion, we conclude that gold mineralization and its associated minerals in the Motongkad prospect are hydrothermal mineralization with epithermal characteristics. We present some facts, especially the dominant type of mineralization in vein and disseminated types. Both types of mineralization are characteristic features of epithermal deposits (e.g., White et al. 1995; Hedenquist et al. 2000; Simmons et al. 2005).

Mineralized hostrock, which is a volcanic rock (andesite and rhyolite lava, as well as tuff), hydrothermal alteration characteristics associated with mineralization as well as ore mineral assemblages associated with gold, such as pyrite, chalcopyrite, sphalerite, tennantite, and supergene minerals such as covellite, chalcocite, and bornite, all also indicate epithermal type mineralization. Textures of mineralized quartz veins, such as vuggy quartz and dog teeth, also characterize this type of epithermal deposit (Dong et al. 1995; Thompson and Thompson 1996; Hedenquist et al. 2000; Einaudi et al. 2003). Previous exploration results around the exploration area also reported the same findings, especially in the Doup and

Lanut Mineralization Districts, which contain epithermal-type mineralization (Kavalieris et al. 1992; Nugroho et al. 2005; van Leeuwen and Pieters 2011, 2012).

The orientation of the veins carrying mineralization in the Motongkad prospect, which is generally trending northwest-southeast (N292°E/4° at ST.1 and N325°E/30° at ST.19), represents the structural control of vein formation, which corresponds to the trend direction of the minor fault along the northern arm of the island of Sulawesi (Effendi and Bawono 1997; Darman and Sidi 2000; Hall and Wilson 2000). This mineralized strike vein generally trending northwest-southeast also corresponds to the trend of the regional strike-slip fault zone that controls the formation of gold mineralization in the Lanut District, which borders the Motongkad prospect, namely the Kotamobagu Shear Zone (Flindell 2003). Thus, we conclude that for more detailed exploration, the geological structure and mineralization trend in the Motongkad prospect is trending northwest-southeast.

The results of the atomic absorption spectrometry (AAS) analysis showed that the gold (Au) content ranged from 0.13 to 1.07 g/t, with the highest range being 0.83–1.07 g/t. Meanwhile, the silver content (Ag) is generally low, except for two locations in the central part of the Motongkad prospect, which reach 5–47 g/t; similarly, the overall base metal content is below 0.05%.

Based on the mineragraphic analysis results, we encountered two types of gold-bearing minerals, namely native gold minerals and electrum, which are generally hosted by pyrite. Based on the alteration-mineralization distribution map that we have made (Figure 3), we found the highest grade gold locations in the quartz-sericite and quartz-sericite-clay alteration zones, which range from 0.83–1.07 g/t.

Conclusions

1. Lithologic units of the studied area consist mainly of andesite, rhyolite, and tuff widely distributed in the southern, northern and central part of the research location, successively.
2. Identified hydrothermal alteration assemblages consisting of quartz-sericite, quartz-sericite-clay, quartz-calcite-sericite-chlorite, quartz-calcite-sericite, and quartz-calcite-kaolinite zones locally occur in porphyritic rhyolite, tuff, rhyolite tuff, and porphyritic andesite.
3. Mineralization types occur as vein and disseminated types which contain hypogene ore minerals, namely gold, pyrite, chalcopyrite, sphalerite, bornite, and tennantite, whereas covellite and chalcocite occur as supergene ore minerals.
4. Hydrothermal alteration assemblages, mineralization types and ore mineral assemblages in the Motongkad prospect including its chemical characteristics are typical of hydrothermal mineralization with epithermal characteristics.

The author would like to thank PT Sultan Bobuyotan Jaya for the permission given to conduct research at the location of the mining license.

REFERENCES

- Darman, H. and Sidi, F.H. 2000. *An Outline of the Geology of Indonesia*. Jakarta: Indonesian Association of Geologists publication. Indonesia.
- Dong et al. 1995 – Dong, G., Morrison, G. and Jaireth, S. 1995. Quartz textures in epithermal veins, Queensland-Classification, Origin, and Implication. *Economic Geology* 90, pp. 1841–185, DOI: 10.2113/gsecongeo.90.6.1841.
- Effendi, A.C. and Bawono, S.S. 1997. *Geology Map Sheet Manado, North Sulawesi*. Pusat Geological Research and Development Center, Bandung.
- Einaudi et al. 2003 – Einaudi, M.T., Hedenquist, J.W. and Inan, E.E. 2003. Sulfidation state of fluids in active and extinct hydrothermal systems: transitions from porphyry to epithermal environments. *Society of Economic Geologists*. Special publication 10, pp. 285–313.
- Flindell, P. 2003. *Avocet Mining. Exploration and Development Across Central and Southeast Asia, Australia Institute of Geoscientists (AIG)*. Mineral Exploration Discussion Group (SMEDG). 10 Oct., Sydney, 8pp.
- Hall, R. and Wilson, M.E.I. 2000. Neogene sutures in eastern Indonesia. *Journal of Asian Earth Sciences* 18, pp. 787–814, DOI: 10.1016/S1367-9120(00)00040-7.
- Hedenquist et al. 2000 – Hedenquist, J.W., Arribas, R.A. and Gonzalez-Urien, E. 2000. Exploration for Epithermal Gold Deposits. *Reviews in Economic Geology* 13, pp. 245–277.
- Kavalieris et al. 1992 – Kavalieris, I., van Leeuwen, T.M. and Wilson, M. 1992. Geological setting and style of mineralization, north arm of Sulawesi, Indonesia. *Journal of Southeast* 7(2/3), pp. 113–129.
- Nugroho et al. 2005 – Nugroho, S., Hardjana, I., Susanto, A.D. and Bautista, C.C. 2005. *Notes on the discovery, geology and mining of the Riska gold deposit, North Sulawesi, Indonesia*. [In:] Priatmoko, S., Digdowirogo, S., Nas, C., van Leeuwen, T. and Widjajanto, H. (Eds), *Indonesian Mineral and Coal Discoveries*, IAGI Special Issues, pp. 31–44.
- Simmons et al. 2005 – Simmons, S.F., White, N.C. and John, D.A. 2005. *Geological characteristics of epithermal precious and base metal deposits*. *Society of economic geologists*. [In:] *Economic geology 100th Anniversary volume*, pp. 485–522.
- Thompson and Thompson 1996. *Atlas of alteration a field and petrographic guide to hydrothermal alteration minerals*. Geological association of Canada mineral deposits division.
- van Leeuwen, T.M. and Pieters, P. 2011. *Mineral deposits of Sulawesi*. Geological agency publication, Ministry of Energy And Mineral Resources, Republic of Indonesia, Bandung.
- White, N.C. and Hedenquist, J.W. 1995. Epithermal gold deposits: styles, characteristics and exploration. *SEG Newsletter* 23(1), pp. 913, DOI: 10.5382/SEGnews.1995-23.fea.

GEOLOGY AND CHARACTERISTIC OF EPITHERMAL GOLD MINERALIZATION AT THE MOTONGKAD PROSPECT, NORTH SULAWESI, INDONESIA

Keywords

epithermal, gold, mineralization, Motongkad, Indonesia

Abstract

In the Motongkad prospect, East Bolaang Mongondow Regency, North Sulawesi Province, Indonesia, an epithermal gold mineralization occurred, hosted in andesitic-basaltic breccia, lava and tuff members the middle Miocene volcanic rock (*Tmv*). The Volcanic Rock is intruded by andesite dikes and contains fine quartz veins. Gold, silver, and pyrite found in the quartz veins.

This study consists of two main stages, field works and laboratory works. The field works were performed in whole area of the Motongkad prospect, where fresh and altered rock and mineralization samples were collected randomly, selectively, and systematically from outcrops as well as from a test pit. The laboratory works include petrography, X-ray diffraction (XRD), ore microscopy, and chemical analysis using the atomic absorption spectrometry (AAS) method.

The study area is arranged by three lithology units. Stratigraphically, the units are andesite rhyolite and tuff. The hydrothermal alteration in the study area are classified in five zones, namely: quartz-sericite, quartz-sericite-clay, quartz-calcite-sericite-chlorite, quartz-calcite-sericite, and quartz-calcite-kaolinite. Motongkad prospect mineralization consists of two types, namely the vein type and the disseminated type. The ore minerals found in the Motongkad prospect are gold, pyrite, chalcopyrite, sphalerite, covellite, chalcocite, bornite and tennantite. We conclude that gold mineralization and its associated minerals in the Motongkad prospect are hydrothermal mineralization with epithermal characteristics.

Based on the results of mineragraphic analysis, there are two types of gold-bearing minerals found, namely native gold minerals and electrum, which are generally hosted by pyrite. Based on the distribution map of alteration and mineralization that has been made, it is recommended that the company wish to conduct mining with the highest gold content in the quartz-sericite and quartz-sericite-clay alteration zones, which are in the range of 0.83–1.07 g/t.

GEOLOGIA I CHARAKTERYSTYKA MINERALIZACJI ZŁOTA EPITERMALNEGO W PROSPEKCIE MOTONGKAD W PÓLNOCNYM SULAWESII, INDONEZJA

Słowa kluczowe

epitermiczny, złoto, mineralizacja, Motongkad, Indonezja

Streszczenie

W prospekcji Motongkad w reencji East Bolaang Mongondow w prowincji Północne Sulawesii w Indonezji miała miejsce epitermalna mineralizacja złota, zlokalizowana w andezytowo-bazaltowej brekcji, lawy i tufie należących do środkowioceńskiej skały wulkanicznej (*Tmv*). Skała wulkaniczna jest intruzją andezytu i zawiera drobne żyły kwarcowe. W żyłach kwarcu znaleziono złoto, srebro i piryt.

Badania te składają się z dwóch głównych etapów, prac terenowych i prac laboratoryjnych. Prace terenowe prowadzono na całym obszarze prospektu Motongkad, gdzie losowo, selektywnie i systematycznie pobierano próbki świeżych i zmienionych skał oraz mineralizacji z wychodni oraz z wykopu badawczego. Prace laboratoryjne obejmują petrografię, dyfrakcję rentgenowską (XRD), mikroskopię rudy oraz analizę chemiczną metodą atomowej spektrometrii absorpcyjnej (AAS).

Obszar badań uporządkowany jest według trzech jednostek litologicznych. Stratygraficznie jednostkami są andezyt, ryolit i tuf. Zmiany hydrotermalne na badanym obszarze sklasyfikowano w pięciu strefach: kwarcowo-serycytowa, kwarcowo-serycytowo-gliniasta, kwarcowo-kalcytowo-serycytowo-chlorynowa, kwarcowo-kalcytowo-serycytowa i kwarcowo-kalcytowo-kaolinitowa. Mineralizacja prospektu Motongkad składa się z dwóch typów, mianowicie typu żyłnego i typu

rozproszonego. Minerale rudne występujące w prospekcji Motongkad to: złoto, piryt, chalkopiryt, sfaleryt, kowelit, chalkozyn, bornit i tennantyt. Doszliśmy do wniosku, że mineralizacja złota i związane z nią minerały w prospekcji Motongkad są mineralizacją hydrotermalną o właściwościach epitermicznych.

Na podstawie wyników analizy mineralogicznej stwierdzono, że istnieją dwa rodzaje minerałów złotonośnych, mianowicie rodzime minerały złota i elektrum, w których zazwyczaj występuje piryt. Na podstawie sporządzonej mapy rozmieszczenia zmian i mineralizacji rekomenduje się, aby spółka prowadziła wydobycie o najwyższej zawartości złota w strefach zmian kwarcowo-serycytowych i kwarcowo-serycytowo-gliniastych, które mieszczą się w granicach 0,83–1,07 g/Mg.